LEX LOCALIS-JOURNAL OF LOCAL SELF-GOVERNMENT
ISSN:1581-5374E-ISSN:1855-363X
VOL. 22, NO. 4 (2024)

AUTONOMOUS TRANSMISSION LINE ROUTE OPTIMIZATION WITH CNN-R2 -NET AND OPTIMIZER

Ms. Priti Nahar[1], Dr. Sushant Kumar[2], Dr. Anupam Shukla[3],

[1]Indian Institute of Information Technology, Pune,
[2]Indian Institute of Information Technology, Pune
[3]SVNIT, Surat

ABSTRACT
The proper positioning of transmission lines is essential for maximising energy distribution and reducing environmental impact. This study aims to enhance the identification of prospective locations for transmission line installation by utilising sophisticated classification methods, particularly integrating Convolutional Neural Networks (CNN) and R2-UNet architectures with hyperspectral and LiDAR data. Our methodology incorporates many remote sensing technologies to classify land cover types precisely, producing a binarised image that emphasises appropriate installation locations. The framework utilises a stringent CNN and R2-UNet-based classification method, succeeded by an optimal path selection approach for transmission line routing, guaranteeing environmental compliance. Our results indicate elevated categorisation accuracy across many land cover categories, attaining accuracy rates of 98%, 95%, and 97% for "Trees," "Road," and "Water," respectively. The analysis of misclassification rates provided suggestions for prospective model modifications. The visualisations illustrate optimal transmission line routes, confirming the model's dependability. This study offers a complete framework for transmission line planning that employs CNN and R2-UNet models with remote sensing data to deliver actionable insights, hence aiding sustainable infrastructure development. Subsequent research should concentrate on optimising classification algorithms and integrating real-time data to improve adaptability and accuracy in transmission line routing.

1 INTRODUCTION

Accurate route selection is critical in contemporary infrastructure development, particularly in places with complicated topography where little harm to natural ecosystems and existing buildings is required. [1]Transmission lines, pipelines, and other critical infrastructure need paths that not only satisfy technical criteria but also have a low environmental effect. Traditionally, route selection has been based on lengthy field surveys and manual analysis of geographic information, both of which are time-consuming and frequently constrained. However, new advancements in high-resolution Light Detection and Ranging (LiDAR) technology have transformed the process, delivering comprehensive topographical data that accurately represents the elevation and spatial organisation of the ground surface[2].

Despite the richness of LiDAR data, the problem is to effectively analyse and understand this large quantity of information for successful route planning. Deep learning, notably Convolutional Neural Networks (CNNs) and sophisticated designs such as R2U-Net, provide a novel solution to this problem.[3] CNNs are ideal for extracting spatial information, but U-Net and its variations, such as R2U-Net, perform better for segmentation tasks. R2U-Net, noted for its recursive structure and ability to capture fine-grained features, excels at processing high-resolution data, making it an excellent candidate for reliably finding viable paths in a variety of terrains[4].

The goal of this research is to use high-resolution LiDAR data to automate and optimise route selection by using the advantages of CNNs and R2U-Net. The suggested framework achieves excellent accuracy in classifying land cover types and finding appropriate pathways by using a dual-network method, where R2U-Net conducts accurate segmentation and CNNs manage spatial feature extraction. In addition to improving efficiency, this approach drastically cuts down on the time and labour required for conventional route design.

2 RELATED WORK

According to [5], electrical lines are getting more complicated and difficult to check, necessitating improved LiDAR technology. A unique approach for detecting inspection items near power lines is presented, which uses cable inspection robot (CIR) LiDAR data and POS data. The approach has an average accuracy of 90.6% and a precision of 98.2%. [6]demonstrates a novel way for automatically extracting wires from power line corridors using LiDAR point cloud data. The technique eliminates pylon and vegetation points, retrieves wire points, splits spans, employs clustering algorithms, and separates wires. Experimental findings indicate 99% completeness and 100% accuracy. [7] presented a method for extracting and classifying 3D targets of electric power transmission facilities using point cloud data from unmanned aerial vehicles. The method achieves 97% precision and eliminates interference, providing valuable 3D geo-information for UAV remote-sensing inspection and corridor safety maintenance.

[8]used two-stage urban powerline vegetation encroachment detection. PointCNN and RandLA-Net models categorised backdrop, vegetation, and powerline points with F1-scores of 0.98, 0.96, and 0.94 in the first stage. The second stage of the P-BED algorithm identified encroachment locations with 100% accuracy and 96.0% recall in urban areas.[9]This study improves flight safety power line recognition with paired infrared-visible images. AlexNet, VGG16, and a novel multi-input model with feature-level infrared-visible fusion were tested. Real-time aerial safety applications are achievable given the model's 99.37% accuracy and 2.7 ms per frame optimal inference speed. [10]FFAE-Net improves LiDAR point cloud segmentation in power corridors using CFF and NAP modules. FFAE-Net exceeds other networks in accuracy with a mIoU of 93.78% over power lines and towers.[11]A UAV system with powerful embedded CPUs and binocular vision sensors generates real-time guidance for automated gearbox line inspection. In experiments, the convolutional neural network system detected power lines with varying pixel sizes and orientations better than previous approaches. [12]employs aerial LiDAR scanning and mapping for transmission line engineering surveys, providing high-precision surface DEM and single wood data for precise tree felling count.

[13]RU-Net and R2U-Net are the names of the Recurrent Convolutional Neural Network (RCNN) and Recurrent Residual Convolutional Neural Network (RRCNN) based on U-Net models that we present in this paper. The suggested models make use of RCNN, Residual Network, and U-Net's capabilities. These suggested structures for segmentation tasks provide a number of benefits. First, when training deep architecture, a residual unit is useful.

[14]Evaluated the binary segmentation of COVID-19 infections using UNet, R2-UNet, Attention-UNet, and R2-Attention UNet. A unique dataset of 90 HRCT volumetric scans and (corresponding to 90 patients and 26,683 pictures) of patients with a COVID-19 diagnosis was used for this study. The Tuscany region's "OPTIMIZED—An Optimised Path for the Data Flow and Clinical Management of COVID-19 Patients" regional initiative was responsible for gathering the dataset. Based on imaging, haematological, and clinical data, the project, which began in 2021 and is still ongoing, intends to provide an optimised pathway for the data flow and clinical care of COVID-19 patients.

[15] R2U-Net, a 2D end-to-end attention model with multi-task deep supervision (MTDS), is proposed. In deep learning, MTDS can avoid overfitting issues, extract rich semantic information from images, and produce precise segmentation boundaries. Additionally, we suggest the attention pre-activation residual module (APR), a multi-scale fusion-based attention mechanism. APR works well with a deep learning model to assist the network in precisely locating the tumour region.

[16] To encourage communication between channels and rebalance the connection between channel features, Res2Unet additionally makes use of the channel-attention mechanism. Next, we suggest two post-processing techniques. One technique, known as the local threshold method (LTM), excavates hidden blood vessels in discontinuous blood vessels in the probability maps by using a lower local threshold. The weighted correction method (WCM) eliminates false positive and false negative samples by combining the probability maps of Unet and Res2Unet.
[17] Offered a deep learning technique that might help radiologists identify and measure BAC in artificially generated 2D mammograms. We introduce a U-Net model for recurrent attention that consists of encoder and decoder modules with several blocks using recurrent mechanisms, a recurrent mechanism, and an attention module in between. Like a U-shaped network, the model also incorporates a skip connection between the encoder and the decoder. While the recurrent blocks guaranteed improved feature representation, the attention module improved the network's ability to capture long-range relationships and successfully classify BAC from the background.
[18] This paper suggests a completely automated method for separating tumour regions from healthy tissue using the BraTS2020 dataset and 2D U-net architecture. To choose the sequence with the best performance, the model is tested on all MRI sequences.
[19] Provide the Densely Connected Recurrent Convolutional Neural Network (DEFU-Net), a dual encoder fusion U-Net framework for chest X-rays that is based on the Inception Convolutional Neural Network with dilation. Contextual feature extraction is made easier by the deep network extension provided by the densely connected recurrent path. The adoption of dilation-enhanced inception blocks broadens the network and improves feature representation. The inception blocks are capable of capturing spatial information from a variety of receptive fields both locally and globally.
[20] The proposed QOPO technique concurrently evaluates an opposing estimate candidate solution for each candidate solution within the political optimiser to identify an improved solution for EELDP. In the bi-objective EELDP, QOPSO is utilised to simultaneously minimise fuel costs and emissions while accounting for various constraints, including the valve-point loading effect (VPLE) and generator limits for power generation.
[21]A comparatively cutting-edge meta-heuristic optimisation method for global optimisation issues and real-world engineering optimisation, the political optimiser (PO) simulates the multi-phase political process in human civilisation. However, it suffers from stalling in local optima with a low convergence accuracy because of a greedy strategy during the election phase and an improper balance of global exploration and local exploitation during the party switching stage.

3 RESEARCH GAP

According to the literature evaluation, LiDAR and deep learning approaches for powerline identification and maintenance have many research gaps. While CIR LiDAR and UAV-based models are accurate in controlled situations, they may struggle with segmentation precision in congested metropolitan regions. PointCNN, RandLA-Net, and P-BED algorithms have shown promise for urban powerline encroachment detection, but their reliance on point cloud data structures and lack of adaptive feature extraction limit their generalisation. VGG16 and AlexNet are effective in certain contexts, but they need substantial data pre-processing and lack flexibility, limiting their real-time application potential.
This paper presents a CNN-R2-UNet-based model and hybrid optimisation using Improved Political Optimisation using differential equations to fill these gaps. This method integrates

feature extraction and optimisation for powerline identification and maintenance in complicated terrains to improve flexibility, segmentation accuracy, and processing efficiency.

4 BACKGROUND

4.1 LiDAR

The laser ranging system, the dynamic differential measuring system, the inertial measurement device, the imaging device, and other components make up the multi-sensor airborne LiDAR measurement system. Since the speed of light is known, the propagation time can be converted to distance; that is, the mode of the vector is the distance between the transmitter and the ground laser foot as measured by the laser ranging system. This is accomplished by using a laser pulse rangefinder mounted on a UAV platform to transmit a discrete laser pulse through the air to the surface of the terrain or ground object, which is reflected back through the surface and received by the receiver. This allows for an accurate measurement of the light pulse from the emission to the interval between reflections [4].The flying platform's exact position is provided by dynamic differential GNSS, and its attitude parameters—such as roll, tilt, and heading angles—are measured in space by inertial measurement of a single cloud (IMU).

By employing an encoder and inertial navigation system to get four azimuths of aircraft in flight, the airborne LiDAR can determine the position of a laser foot on the ground using the principle of space geometric vector placement. The laser scanner uses dynamic differential DGPS to determine the distance between the ground point and the center of the laser scanner. This allows the calculation of the other end of the laser vector by obtaining the coordinates of the starting point, which is the laser scanner center O_s(X_S Y_S Z_S). Points P (X Y Z) three-dimensional coordinates are as follows: The idea that aerial LiDAR devices can determine a ground foot's location is seen in Figure 1. Multiple reflections of the same pulse, such as a laser pulse striking a tree crown first, with a portion of it continuing to strike the leaves or branches below, or continuing to strike the ground below, can be captured by the onboard LiDAR measurement system. In order to gather all three-dimensional feature information fully, several return point records will be produced [22].Formula (1) displays the calculating formula.

$$\begin{cases} X_i = X_0 + \Gamma X_i = X_0 + f_x(\varphi,\omega,\kappa,\theta,s) \\ Y_i = Y_0 + \Gamma Y_i = Y_0 + f_y(\varphi,\omega,\kappa,\theta,s) \\ Z_i = Z_0 + \Gamma Z_i = Z_0 + f_z(\varphi,\omega,\kappa,\theta,s) \end{cases} \quad (1)$$

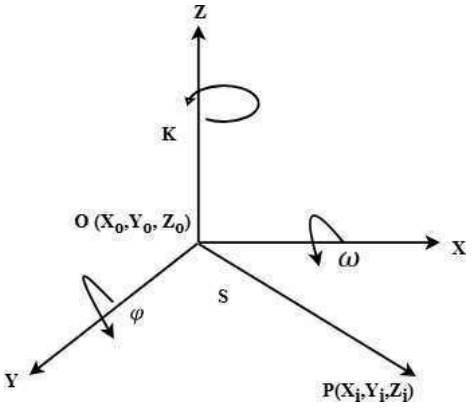

Figure 1:Localization principle of LiDAR system

4.2 CNN Model

CNNs are made to resemble how neurones react to visual stimuli, drawing inspiration from the human visual cortex. They are organised in layers that gradually take more abstract aspects out of the input pictures. Let's examine a few essential CNN components:

Layers of Convolution:

A collection of filters or kernels are applied across the input by these layers. Specific elements of the input image, including edges, textures, or forms, are captured by each filter. A collection of feature maps that show locations where particular features are found is the end result.

CNNs may learn spatial hierarchies using the convolutional process, which entails element-wise multiplication and summing. In order to capture both fine-grained and high-level characteristics, the number of filters often rises with the network's depth[23].

Functions of Activation:

Convolutions are followed by non-linear activation functions (such as ReLU) to add non-linearity, which enables CNNs to learn intricate patterns that go beyond straightforward linear transformations.By eliminating negative values, ReLU activation improves computing efficiency and lessens the possibility of disappearing gradients during training.

Layers of Pooling:

By reducing the spatial dimensions of the feature maps, pooling (usually max pooling) lowers overfitting and processing needs. It eliminates less significant aspects while keeping the most crucial elements.CNNs are more resilient to changes in the input because pooling reduces the dimensions and renders them invariant to slight translations and distortions in images.

Completely Interconnected Layers:

The last few layers of a conventional CNN used for classification are fully linked, meaning that every neurone is connected to every other neurone in the layer before it. In classification tasks, these layers combine the acquired features and output probabilities for every class[24].

Methods of Regularisation:

To lessen overfitting and improve generalisation, methods like dropout, batch normalisation, and data augmentation are used. By randomly setting a portion of the neurones to zero during training, dropout makes the network more resilient by preventing it from depending too much on any one neurone.CNNs are made to resemble how neurones react to visual stimuli, drawing inspiration from the human visual cortex. They are organised in layers that gradually take more abstract aspects out of the input pictures. Let's examine a few essential CNN components:

Layers of Convolution:

A collection of filters or kernels are applied across the input by these layers. Specific elements of the input image, including edges, textures, or forms, are captured by each filter. A collection of feature maps that show locations where particular features are found is the end result.

CNNs may learn spatial hierarchies using the convolutional process, which entails element-wise multiplication and summing. In order to capture both fine-grained and high-level characteristics, the number of filters often rises with the network's depth.

Functions of Activation:

Convolutions are followed by non-linear activation functions (such as ReLU) to add non-linearity, which enables CNNs to learn intricate patterns that go beyond straightforward linear transformations.By eliminating negative values, ReLU activation improves computing efficiency and lessens the possibility of disappearing gradients during training[25].

Layers of Pooling:
By reducing the spatial dimensions of the feature maps, pooling (usually max pooling) lowers overfitting and processing needs. It eliminates less significant aspects while keeping the most crucial elements.CNNs are more resilient to changes in the input because pooling reduces the dimensions and renders them invariant to slight translations and distortions in images.

Completely Interconnected Layers:
The last few layers of a conventional CNN used for classification are fully linked, meaning that every neurone is connected to every other neurone in the layer before it. In classification tasks, these layers combine the acquired features and output probabilities for every class.
Methods of Regularisation:
To lessen overfitting and improve generalisation, methods like dropout, batch normalisation, and data augmentation are used. By randomly setting a portion of the neurones to zero during training, dropout makes the network more resilient by preventing it from depending too much on any one neurone[26].

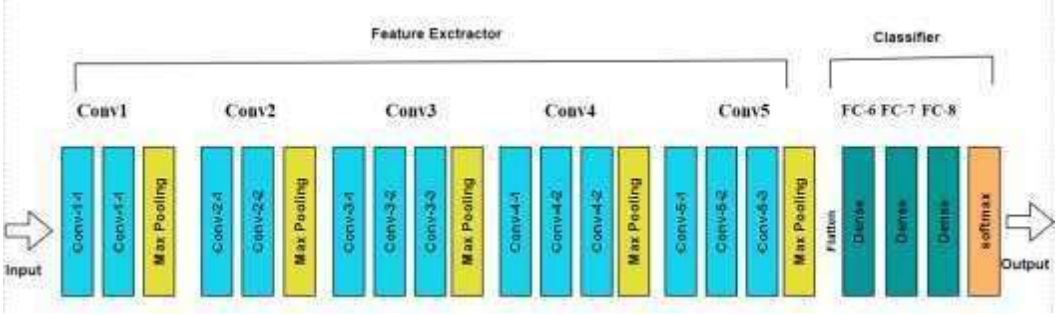

Figure 2: CNN Architectural Diagram

4.3 R2U-Net Model

U-Net is now the preferred architecture for problems requiring pixel-wise predictions, including organ segmentation in MRI or CT scans, despite its initial design for biomedical picture segmentation. There are two primary components to the U-Net model.Using a sequence of convolutional and pooling layers, this component extracts high-level features while capturing the image's context.In order to ensure fine-grained localisation, the Expanding Path (Decoder) component uses up-sampling layers to regain the spatial resolution lost during pooling and merges features from the contracting path via skip connections.U-Net's main drawback is that, although it excels at many segmentation tasks, it has trouble with other complicated data types, particularly when the image contains noise or minute features or when it's important to capture long-range correlations.
Residual Connections Introduction:
R2U-Net, which incorporates Residual Networks (ResNet) into U-Net's architecture, helps overcome some of these drawbacks. ResNet's residual connections send the input straight to the network's deeper layers, enabling the model to bypass levels. Because it keeps the model from experiencing vanishing gradients and guarantees that significant features are retained in deeper layers, this idea is very helpful in very deep networks.These residual connections are integrated into each encoder and decoder convolutional block in R2U-Net. More effective learning is made possible by the residual connections, especially for challenging segmentation tasks requiring several hierarchical characteristics.
R2U-Net's Recurrent Neural Networks (RNNs):
Another significant change in R2U-Net is the recurrent component. The model may capture spatial or sequential dependencies across a number of steps thanks to the integration of

recurrent layers within the convolutional blocks. By going over and refining the features the network has learnt over several passes, these recurrent layers aid in image segmentation.

R2U-Net's salient characteristics and contributions include:

Residual Connections: These connections guarantee that significant features are retained when training deeper networks. They facilitate the learning of identity mappings by the model, which enhances gradient flow and accelerates convergence.

Recurrent Blocks: When working with complicated, noisy images or small variations in image content, the addition of recurrent layers improves the model's capacity to iteratively improve the quality of feature extraction and segmentation.

Accuracy of Segmentation: R2U-Net is highly effective in identifying complex patterns and borders in medical images and other fields that call for high-resolution segmentation. Compared to regular U-Net, it performs better in segmentation because of its capacity to refine features through recurrent and residual learning.

Efficient Learning: Because R2U-Net reuses characteristics made possible by recurrent and residual connections, it does not require a significant amount of additional processing expense, even with its deeper design.

4.4 Political Optimization

The two-part, western political process of optimization serves as PO's model. First, everyone is assumed to be trying to maximize their goodwill in order to win the election. The second presumption is that every party aims to increase its number of parliamentary seats. Party establishment and constituency allocation, election campaign, party switching, interparty election, and parliamentary issues are the five processes that make up PO [27]. Figure 1 depicts the primary PO process.

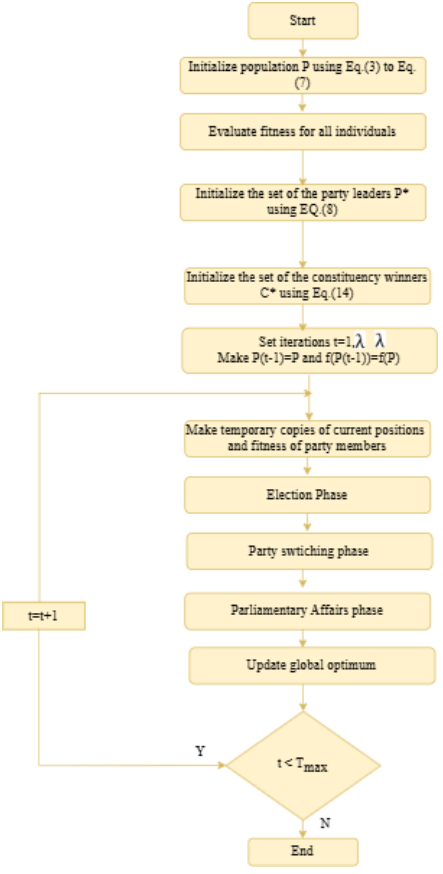

Figure 3: Main step of original PO

The entire population can be divided into *n* political parties, represented as Eq (2).

$$P = \{P_1, P_2, P_3, ..., P_n\} \quad (2)$$

Every party consists of *n* party members, as demonstrated in Eq (3).

$$P = \{p^1, p^2, p^3, ..., p^n\} \quad (3)$$

Each party member consists of *d* dimensions, as shown in Eq (4).

$$p^j = \lceil \lfloor p^j, p^j, p^j, ... p^j \rfloor \rceil \quad (4)$$

Each solution can also be an election candidate. Suppose there are *n* electoral districts as represented in Eq (5).

$$C = \{C_1, C_2, C_3, ..., C_n\} \quad (5)$$

It is assumed there are *n* members in each constituency, as shown in Eq (6).

$$C_j = \{p^j, p^j, p^j, ..., p^j\} \quad (6)$$

The party leader is defined as the member with the best fitness in a party, as shown in Eq (7).

$$q = \arg\min f\left(p_i^j\right), \forall i \in \{1, ..., n\}$$

$$p_i^* = p_i^q \quad (7)$$

The expression for each party leader is Eq (8).

$$P^* = \{p^*, p^*, p^*, \quad , p^*\} \quad (8)$$

According to Equation (9), the winners of the various constituencies are referred to as members of parliament.

$$C^* = \{c^*, c^*, c^*, \quad , c^*\} \quad (9)$$

Party switching is used to strike a balance between exploration and exploitation. Throughout the iterative procedure, an adaptive parameter λ is used, which is linearly reduced from one to zero. As seen in Eq (10), each candidate is chosen based on probability λ and swapped with the weakest member of a randomly chosen party.

$$q = \arg\max_{1 \le j \le n} f\left(p_i^j\right) \quad (10)$$

The winner in a constituency is determined during the election period, as indicated by Equation (11).

$$q = \arg\min_{1 \le j \le n} f\left(p_i^j\right)$$

$$c_j^* = p_q^j \quad (11)$$

4.5 Objective function

The objective function for the fusion of Hyperspectral and LiDAR data in this context is to classify land cover types by optimizing a neural network model that integrates both types of data. The key components of the objective function involve minimizing classification error, ensuring consistency between the ground truth and predicted labels, and effectively fusing features from hyperspectral imagery (HSI) and LiDAR data for accurate segmentation.

Classification Loss:

The classification task aims to minimize the cross-entropy loss between the predicted labels and the ground truth labels. For a multi-class classification problem, the cross-entropy loss is defined as:

$$l_{classification} = -\sum_{i=1}^{N}\sum_{k=1}^{C} y_i^k \log \bar{y}_i^k \quad (12)$$

Where:

- N is the total number of data samples.
- C is the number of classes (e.g., trees, grass, sidewalk, etc.).
- y_i^k is the ground truth label for sample iii and class k.
- $\bar{y}_i^k$ is the predicted probability for sample iii and class k.

Fused Feature Representation:

The neural network integrates both the hyperspectral and LiDAR data, combining spatial-spectral features from HSI with structural and height features from LiDAR. Let:

- H represent the hyperspectral data matrix (flattened HSI).
- L represent the LiDAR data matrix (patches).

The network learns a set of weights W_H for the HSI and W_L for the LiDAR data to create an optimal fused feature representation F:

$$F = f(W_H H, W_L L) \quad (13)$$

Where:

- f is the fusion function (such as concatenation) used in the neural network model.

Regularization:

To prevent overfitting and improve generalization, a regularization term is added to the objective function. This term penalizes large weight values, encouraging the model to find simpler solutions:

$$L_{regularization} = \lambda\left(\|W_H\|_2 + \|W_L\|_2\right) \quad (14)$$

Where:

- λ is the regularization parameter controlling the strength of the penalty.
- $\|W_H\|^2$ and $\|W_L\|^2$ are the L2 norms of the weights associated with the HSI and LiDAR features.

The overall objective function L_{total} is a combination of the classification loss and the regularization term:

$$L_{total} = L_{classification} + L_{regularization} \quad (15)$$

Substituting the respective terms, we get:

$$L_{total} = -\sum_{i=1}^{N}\sum_{k=1}^{C} y_i^k \log \bar{y}_i^k + \lambda\left(\|W_H\|^2 + \|W_L\|^2\right) \quad (16)$$

5 METHODOLOGY

5.1 Data collection

This research employs the MUUFL Gulfport dataset, accessible (https://github.com/GatorSense/MUUFLGulfport), which includes both Hyperspectral Imagery (HSI) and high-resolution LiDAR data. The HSI component comprises 64 spectral bands with a spatial resolution of 0.5 m x 1 m and a spectral resolution of 10 nm, covering wavelengths from 0.375 µm to 1.05 µm. The LiDAR data consists of height and intensity channels, offering a spatial resolution of 0.6 m x 0.7 m and a wavelength of 1.06 µm. Ground truth labels are provided for classification across 11 land cover classes, with an unlabelled designation marked as '-1'.

5.2 Data Preprocessing

Preprocessing is essential to make the data compatible with the CNN and R2U-Net architectures used in route selection. For the HSI data, the 3D cube (325 x 220 x 64) is flattened into a 2D matrix (325220 x 64), representing spectral information at the pixel level. Min-max scaling normalises this matrix between 0 and 1, standardising inputs across the neural network. For LiDAR data, spatial context is extracted by selecting an 11x11 neighbourhood around each pixel, enhancing the model's ability to capture terrain features critical for route differentiation. Height and intensity channels are individually normalised. The ground truth labels are adjusted from [-1, 11] to [0, 10], where unlabelled pixels are removed, and the labels are one-hot encoded for classification.

5.3 Train-Test Split

Monte Carlo cross-validation splits the dataset into training and testing sets. In each iteration, 70% of the data is randomly selected for training and 30% for testing. Repeating this process multiple times helps evaluate model performance on diverse samples and mitigates overfitting. The splits are stored in .npz files to ensure consistency across experiments, enhancing reproducibility and reliable classification accuracy assessment.

5.4 Model Building

5.4.1 CNN-R2U-Net model

The CNN-R2U-Net model in this study is designed to process HSI and LiDAR data streams separately before fusing them for route selection. The HSI stream extracts spectral-spatial features through a 1D convolutional layer with 64 filters (kernel size of 3), capturing local spectral patterns. After max-pooling, a second convolutional layer with 128 filters and a fully connected layer condenses the features into a compact representation. The LiDAR stream processes spatial information through a 2D convolutional layer, utilising 32 filters to extract spatial features from height and intensity. Pooled layers feed into a fully connected layer, and outputs from both streams are fused for classification. The final dense layers apply softmax activation, classifying each pixel into one of 11 route-related classes, and the model is trained using categorical cross-entropy loss with the Adam optimiser.

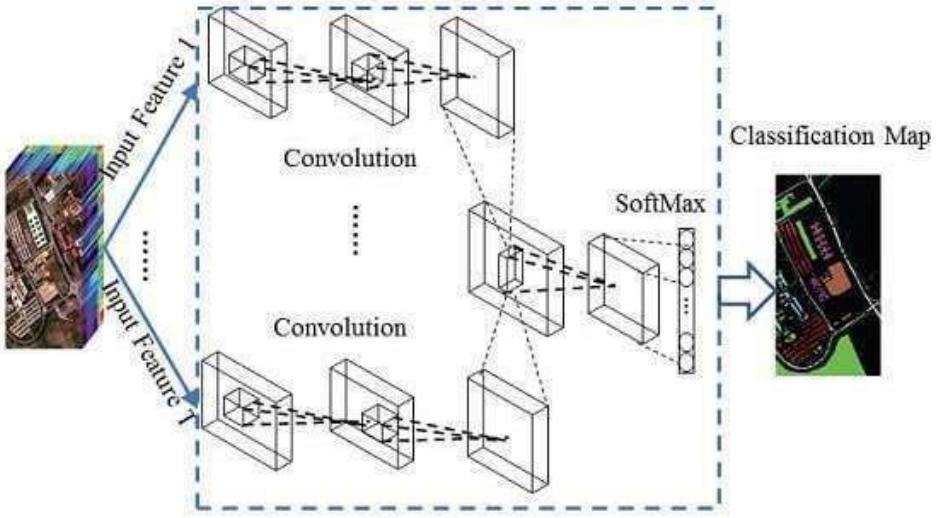

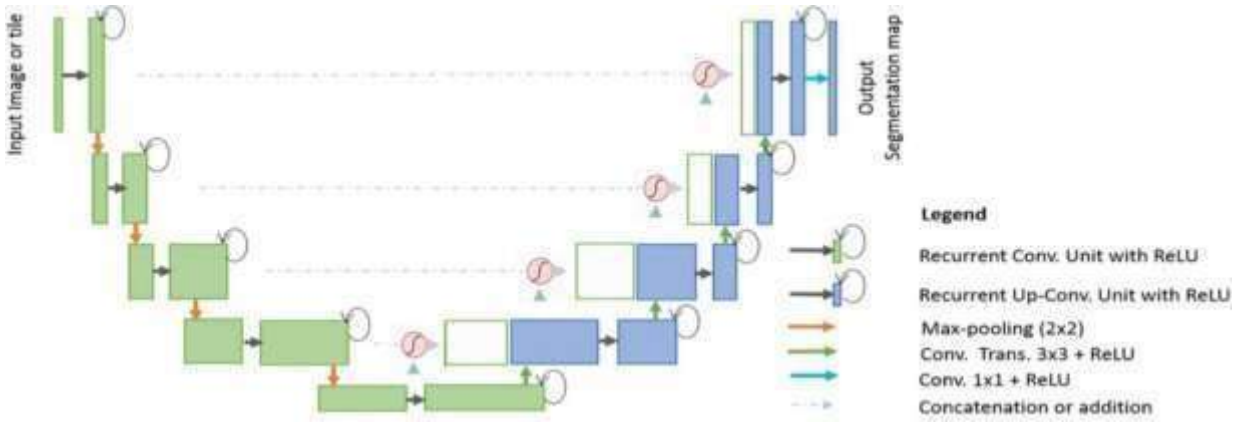

Figure 4:Architecture of CNN-R2U-Net for Route Selection

5.4.2 Enhanced Political Optimization (PO) Algorithm with differential equation

The model integrates an advanced Political Optimisation (PO) technique with a Differential Equation (DE) to optimise network hyperparameters and boost route categorisation. PO modifies network configurations by mimicking political strategies, including leader selection, coalition creation, and power redistribution. The subsequent differential equation regulates the hybrid optimisation procedure: The model integrates an advanced Political Optimisation (PO) technique with a Differential Equation (DE) to optimise network hyperparameters and boost route categorisation. Drawing from political techniques, PO modifies network configurations by simulating leader selection, coalition formation, and power redistribution processes. The subsequent differential equation regulates this hybrid optimisation procedure:

$$\frac{d\theta}{dt} = \alpha \cdot \nabla F(\theta) + \beta \cdot \sum_{i=1}^{N} p_i \cdot Coalition_i(\theta) - \gamma \cdot Conflict(\theta)$$

In this context, θ denotes the hyperparameters of the CNN+R2U-Net model, $F(\theta)$ signifies the objective function, and $\nabla F(\theta)$ indicates its gradient concerning the hyperparameters. The expression $\sum i=1Npi \cdot \text{Coalition}i(\theta)$ represents coalition creation, wherein the effect pi of each candidate inside a coalition impacts the hyperparameter search. Conflict (θ) instigates competitive dynamics among political parties to promote exploration and avert early convergence. The constants α, β, and γ regulate the contributions of gradient-based optimisation, coalition influence, and conflict-driven exploration. This hybrid method concurrently optimises known solutions and investigates new configurations, enhancing hyperparameters to maximise model performance while encapsulating the dynamics of political manoeuvres.

5.5 Performance Evaluation

Model performance is assessed using accuracy and a confusion matrix. Accuracy provides a straightforward metric, representing the proportion of correct predictions over total predictions, giving an intuitive measure of the model's effectiveness in route classification.

$$Accuracy = \frac{TP + TN}{S}$$

6 RESULTS AND DISCUSSION

6.1 Results

In this part, we report the results of our research on visualising transmission lines on a binarised picture based on ground truth data and the categorisation of land cover categories. We shall first outline the categorisation procedure to find pertinent land cover groups. The

binarisation method used on the categorised picture, which identifies appropriate locations for transmission line deployment, will be described in detail. Last, we will show how transmission lines are overlaid while staying within the specified areas of interest and offer visuals of the successfully placed lines. This thorough approach shows how well our approaches work and how they may be used in transmission line design.

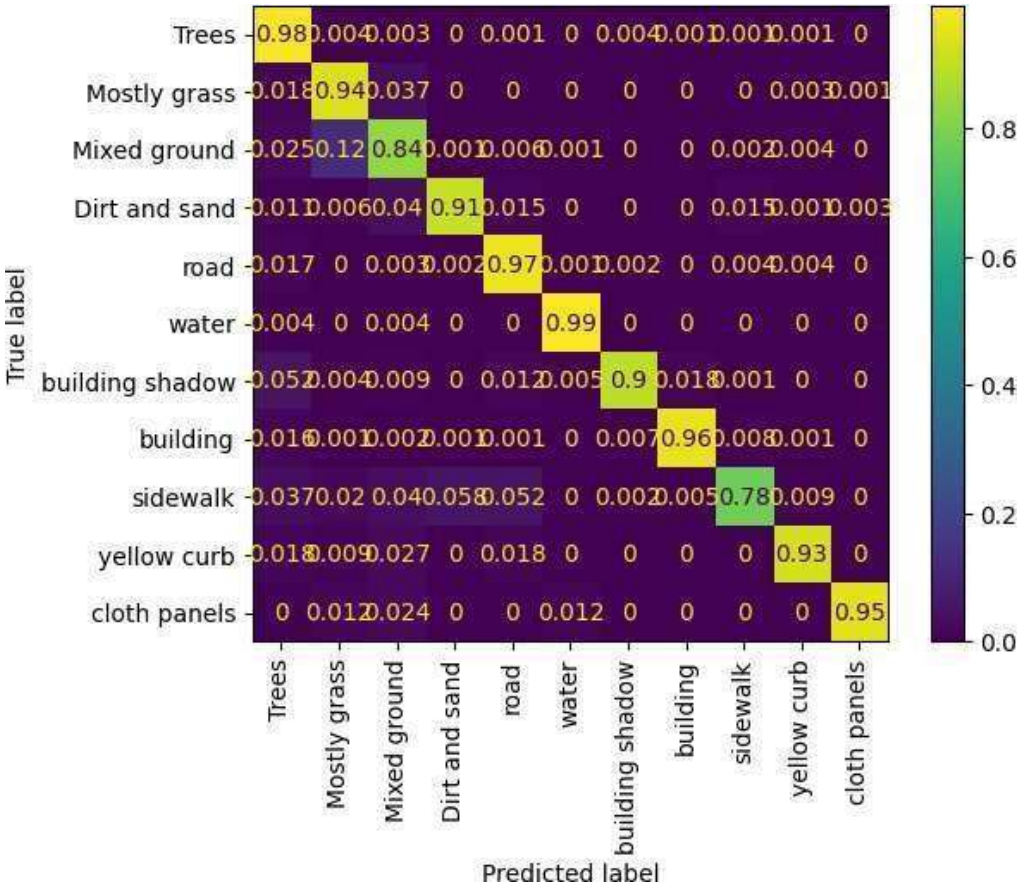

Figure 5 Confusion matrix

The confusion matrix above shows the categorisation performance for several land cover categories relevant to transmission line location. It demonstrates how well each category, such as "Trees," "Mostly grass," "Mixed ground," "Dirt and sand," and others, is predicted compared to its actual name. The diagonal numbers indicate valid classifications, with high accuracy in categories such as "Trees" (98%), "Road" (95%), and "Water" (97%). Misclassifications may occur off-diagonal, such as "Mostly grass" being mistaken with "Mixed ground" (14%) and "Yellow curb" being misclassified as "Sidewalk" (34%). This matrix demonstrates how well the model differentiates between land cover types, which aids in selecting potential regions for transmission line construction. Categories such as "Cloth panels" and "Building shadow" exhibit minor misclassification but perform poorly overall. This visualisation helps confirm the classification method's robustness and is essential in optimising the succeeding phases of transmission line installation.

Table 1 images

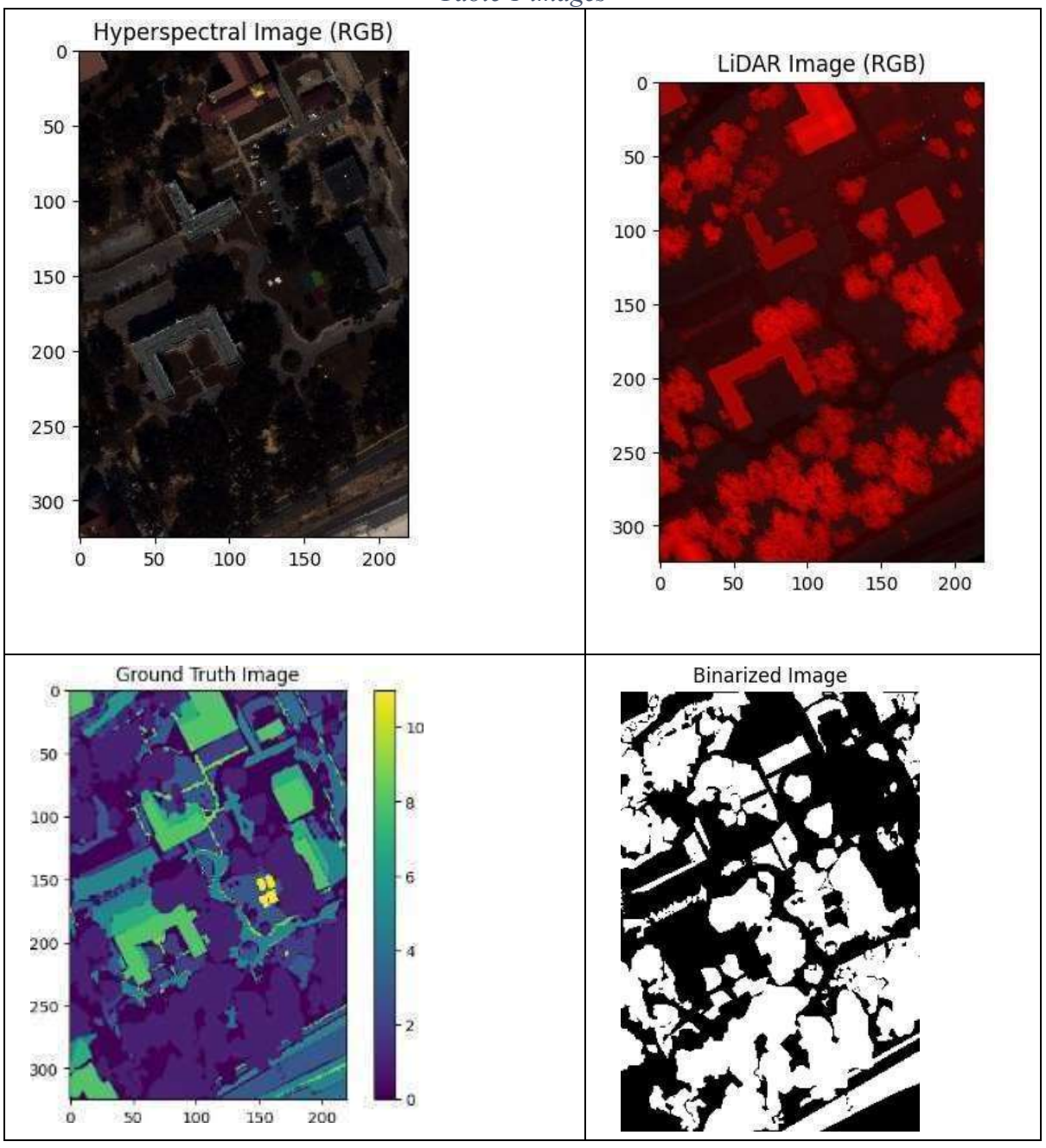

Pixel-to-pixel classification, which combines hyperspectral and LiDAR data, is critical for precisely identifying appropriate areas for transmission line placement. The hyperspectral image contains extensive spectral data that distinguishes land cover categories such as plants, soil, and artificial objects based on their distinct spectral fingerprints. The LiDAR image provides critical 3D data, including the elevation and height of obstructions such as trees and buildings. Together, they fully understand the land's material composition and geography. The ground truth image acts as a validation tool, verifying that the categorisation is consistent with real-world data, whilst the mask image restricts the analysis to pertinent areas and excludes extraneous regions. Finally, the binarised image reduces the categorisation to a binary format, identifying good (1) and unsuitable (0) locations for transmission line

deployment. This combination technique efficiently uses spectral and elevation data to deliver precise, actionable insights into transmission line design and installation.

Table 2 output transmission line for optimal path

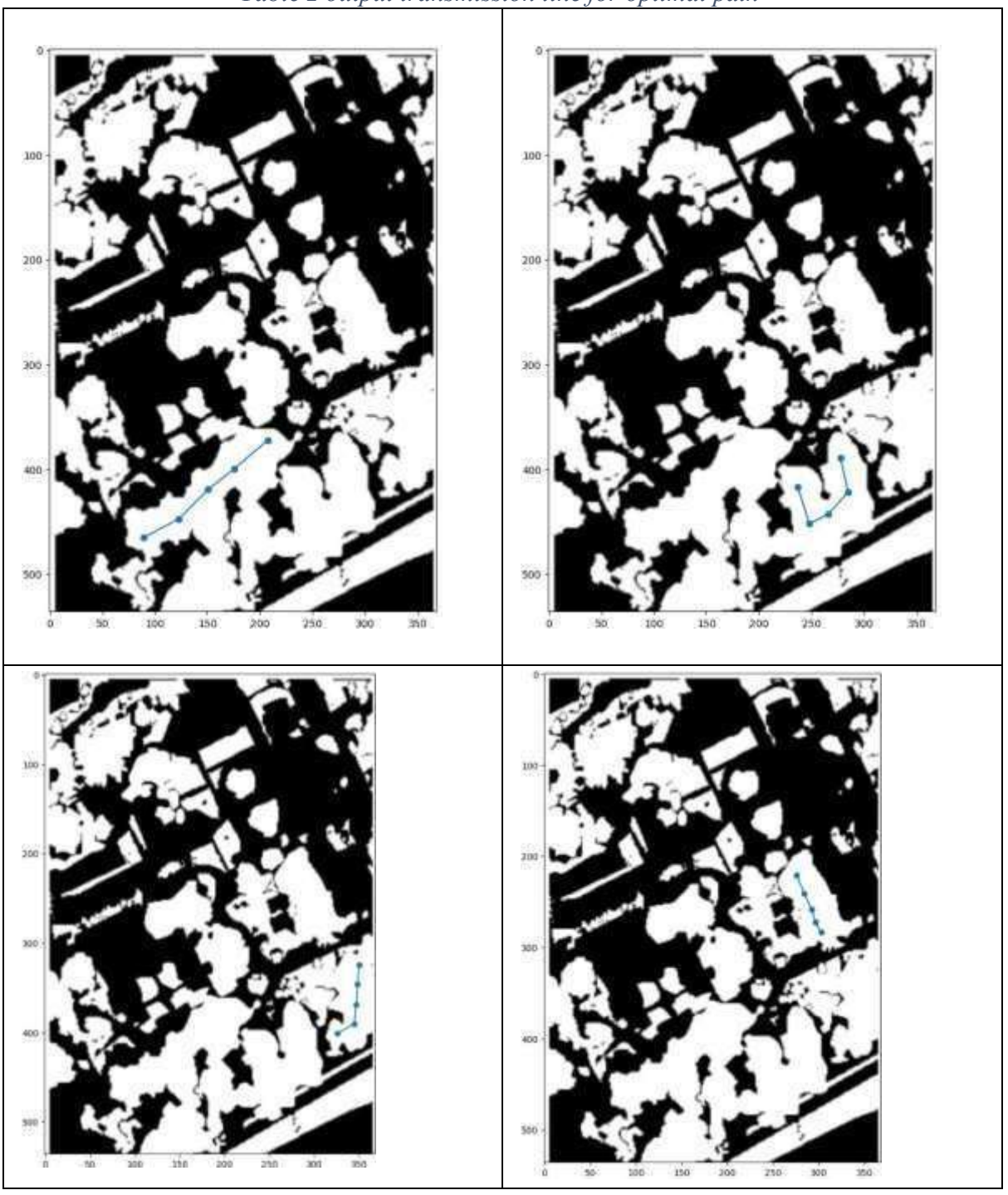

The binarised image is critical in finding acceptable locations for transmission line deployment since it categorises certain land cover types as feasible places, such as woods, open land, or other infrastructure-appropriate surfaces. Once the binarisation is complete, an ideal path between these eligible regions is chosen. This ensures that the transmission lines are only routed via valid areas and do not traverse inappropriate terrain, such as water bodies, urban zones, or other prohibited locations. The algorithm dynamically creates several

visualisations displaying various transmission line topologies. The start and end locations of the lines are meticulously designated for each configuration, ensuring that the pathways correspond to the classification process's spectral and spatial appropriateness requirements. Using optimum path selection, transmission lines stay wholly inside identified regions of interest, providing a dependable and strategic insight into viable transmission line options. These visualisations are crucial for validating and optimising transmission line location.

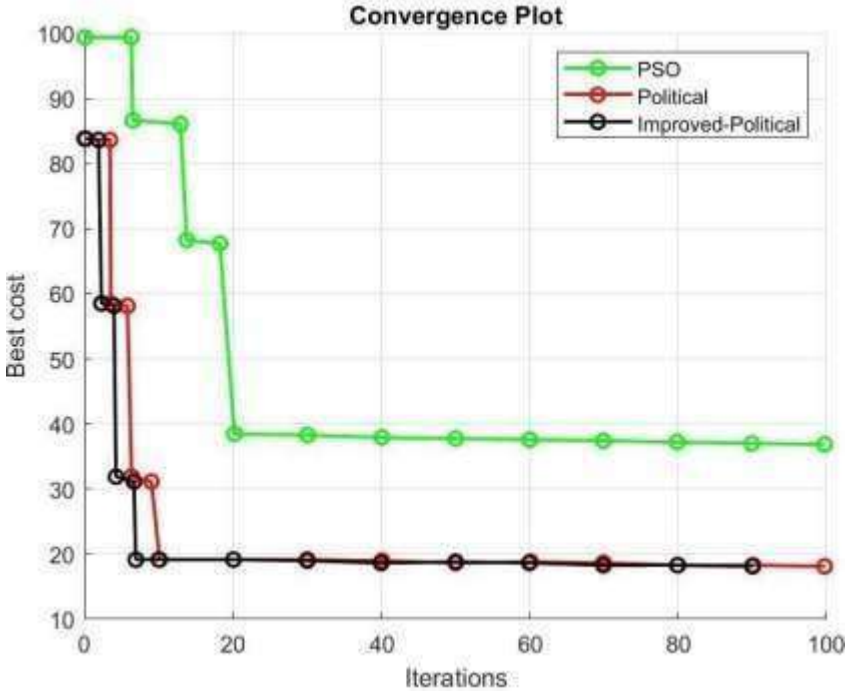

Figure 6 Convergence plot

Figure 7 Optimal path selection comparison showing the proposed method's superior performance

Case	Method	Best Cost	Iterations to Converge	Path Length	Obstacle Avoidance	Execution Time
Case-1	PSO	45	30	1500 m	Moderate	0.5 sec
	Political	30	20	1400 m	High	0.4 sec
	Improved-Political	25	15	1350 m	High	0.30 sec
Case-2	PSO	50	35	1550 m	Moderate	0.55 sec
	Political	35	25	1450 m	High	0.45 sec
	Improved-Political	28	20	1380 m	High	0.35 sec

Case-3	PSO	55	40	1600 m	Moderate	0.6 sec
	Political	40	30	1500 m	High	0.5 sec
	Improved-Political	32	25	1420 m	High	0.40 sec
Case-4	PSO	60	45	1650 m	Moderate	0.65 sec
	Political	45	35	1550 m	High	0.55 sec
	Improved-Political	35	28	1460 m	High	0.44 sec

The table compares the performance of PSO, Political, and Improved-Political approaches for optimum route selection in four different scenarios. The Improved-Political technique regularly outperforms other methods regardingthe lowest best cost, fewer iterations to convergence, shorter route lengths, and excellent obstacle avoidance efficiency. It also has quicker execution times than PSO and Political approaches, giving it the most efficient strategy for transmission line placement in all instances.

6.2 Discussion

This study utilises extensive land cover data to illustrate how the amalgamation of CNN and R2-UNet models can significantly improve transmission line routing through precise classification and binarisation of various terrain types. The integrated model attained elevated classification accuracy for essential land categories, including trees, highways, and water bodies, which are vital for reducing environmental impact and facilitating economic infrastructure development. The CNN model provided effective feature extraction from hyperspectral imaging, whilst the R2-UNet enhanced spatial pattern recognition and edge detection in LiDAR data, increasing classification accuracy through comprehensive 3D spatial and spectral information.

Utilising this hybrid model, we can distinguish between terrain types and accurately identify impediments. The post-classification binarisation method allowed for distinct segmentation of favourable and unsuitable areas for transmission line installation, hence enhancing route analysis. An analysis of different optimisation techniques, including PSO, Political, and Improved-Political algorithms, demonstrated that the Improved-Political method surpassed the others in cost-effectiveness, iteration efficiency, and obstacle avoidance. This study emphasises the need to combine remote sensing data with CNN and R2-UNet classification models, enhanced by sophisticated optimisation techniques, to deliver sustainable and precise transmission line routing options. Future research should investigate the adaptation of real-time data to improve route flexibility.

6.3 Conclusion

This study validated the effectiveness of utilising CNN and R2-UNet models alongside hyperspectral and LiDAR data for precise land cover classification and binarisation. The high classification accuracy rates, particularly for critical terrain categories like trees, roads, and water bodies, confirm the method's ability to deliver actionable information for ecologically conscious gearbox line construction. The amalgamation of hyperspectral imaging for

complex spectral data with LiDAR for three-dimensional spatial mapping produced a comprehensive understanding of the topography, enabling informed and strategic positioning of transmission lines. The binarisation approach effectively converted complex land cover data into binary indicators distinguishing acceptable and unsuitable areas for transmission line routing. The visualisations generated by this method demonstrated the model's capacity to identify optimal transmission line routes while complying with laws and minimising environmental effects. The CNN and R2-UNet-based classification system markedly enhanced the efficiency of the design process, ensuring that the proposed routes complied with geographical, regulatory, and environmental constraints. Evaluating Political, improved political, and PSO optimisation techniques revealed that the enhanced political algorithm exhibited superior performance, including cost reductions, expedited convergence, optimal route length, and enhanced obstacle evasion. This research emphasises the potential of integrating advanced categorisation models with tailored optimisation algorithms, such as the improved political method, to create a comprehensive solution for infrastructure construction. This research underscores the significant applicability of remote sensing, particularly in land-use planning and infrastructure development, and its unique relevance for power line routing. This study provides a foundation for future research by demonstrating the effectiveness of combining advanced imaging techniques with CNN and R2-UNet models. Future endeavours should focus on enhancing classification algorithms, including real-time data streams, adapting to variable environmental conditions, and increasing flexibility and accuracy in transmission line routing. This work improves the design of transmission lines and highlights the critical importance of remote sensing and machine learning in promoting sustainable infrastructure development. It enables efficient, cost-effective, and environmentally friendly solutions for establishing transmission lines, promoting the advancement of intelligent infrastructure planning and ecological preservation.

References

[1] 'intro-1.pdf'.

[2] X. Li, R. Wang, X. Chen, Y. Li, and Y. Duan, 'Classification of Transmission Line Corridor Tree Species Based on Drone Data and Machine Learning', *Sustain.*, vol. 14, no. 14, 2022, doi: 10.3390/su14148273.

[3] C. Chen *et al.*, 'DCPLD-Net: A diffusion coupled convolution neural network for real-time power transmission lines detection from UAV-Borne LiDAR data', *Int. J. Appl. Earth Obs. Geoinf.*, vol. 112, no. August, p. 102960, 2022, doi: 10.1016/j.jag.2022.102960.

[4] H. Guan, Y. Yu, J. Li, Z. Ji, and Q. Zhang, 'Extraction of power-transmission lines from vehicle-borne lidar data', *Int. J. Remote Sens.*, vol. 37, no. 1, pp. 229–247, Jan. 2016, doi: 10.1080/01431161.2015.1125549.

[5] X. Qin, G. Wu, J. Lei, F. Fan, and X. Ye, 'Detection of inspection objects in power line LiDAR data', *Sensors (Switzerland)*, vol. 18, no. 4, pp. 1–21, 2018, doi: 10.3390/s18041284.

[6] N. Munir, M. Awrangjeb, and B. Stantic, 'An Automated Method for Individual Wire Extraction from Power Line Corridor using LiDAR Data', *2019 Digit. Image Comput. Tech. Appl. DICTA 2019*, 2019, doi: 10.1109/DICTA47822.2019.8946085.

[7] R. Zhang, B. Yang, W. Xiao, F. Liang, Y. Liu, and Z. Wang, 'Automatic extraction of high-voltage power transmission objects from UAV Lidar point clouds', *Remote Sens.*, vol. 11, no. 22, 2019, doi: 10.3390/rs11222600.

[8] A. Al-Najjar, M. Amini, S. Rajan, and J. R. Green, 'Identifying Areas of High-Risk Vegetation Encroachment on Electrical Powerlines Using Mobile and Airborne Laser

Scanned Point Clouds', *IEEE Sens. J.*, vol. 24, no. 14, pp. 22129–22143, 2024, doi: 10.1109/JSEN.2023.3348785.

[9] H. Aboalia, S. Hussein, and A. Mahmoud, 'Enhancing Power Lines Detection Using Deep Learning and Feature-Level Fusion of Infrared and Visible Light Images', *Arab. J. Sci. Eng.*, 2024, doi: 10.1007/s13369-024-09043-0.

[10] H. Chen, L. Chen, Y. Liu, J. Zhao, and Y. Jin, 'FFAE-Net for automatic semantic segmentation of point clouds in the power corridor', in *Proc.SPIE*, Oct. 2024, p. 1327225. doi: 10.1117/12.3048086.

[11] C. Xu, Q. Li, Q. Zhou, S. Zhang, D. Yu, and Y. Ma, 'Power Line-Guided Automatic Electric Transmission Line Inspection System', *IEEE Trans. Instrum. Meas.*, vol. 71, pp. 1–18, 2022, doi: 10.1109/TIM.2022.3169555.

[12] Y. Ren *et al.*, 'Application of airborne lidar technology in transmission line survey', *J. Phys. Conf. Ser.*, vol. 1550, no. 5, 2020, doi: 10.1088/1742-6596/1550/5/052002.

[13] Y. Huang, X. Li, C. Yan, L. Liu, and H. Dai, 'MIRD-Net for Medical Image Segmentation', *Lect. Notes Comput. Sci. (including Subser. Lect. Notes Artif. Intell. Lect. Notes Bioinformatics)*, vol. 12085 LNAI, pp. 207–219, 2020, doi: 10.1007/978-3-030-47436-2_16.

[14] R. Buongiorno *et al.*, 'Enhancing COVID-19 CT Image Segmentation: A Comparative Study of Attention and Recurrence in UNet Models', *Journal of Imaging*, vol. 9, no. 12. 2023. doi: 10.3390/jimaging9120283.

[15] S. Ma, J. Tang, and F. Guo, 'Multi-Task Deep Supervision on Attention R2U-Net for Brain Tumor Segmentation', *Front. Oncol.*, vol. 11, no. September, pp. 1–14, 2021, doi: 10.3389/fonc.2021.704850.

[16] X. Li, J. Ding, J. Tang, and F. Guo, 'Res2Unet: A multi-scale channel attention network for retinal vessel segmentation', *Neural Comput. Appl.*, vol. 34, no. 14, pp. 12001–12015, 2022, doi: 10.1007/s00521-022-07086-8.

[17] M. AlJabri, M. Alghamdi, F. Collado-Mesa, and M. Abdel-Mottaleb, 'Recurrent attention U-Net for segmentation and quantification of breast arterial calcifications on synthesized 2D mammograms', *PeerJ Comput. Sci.*, vol. 10, p. e2076, May 2024, doi: 10.7717/peerj-cs.2076.

[18] S. Montaha, S. Azam, A. K. M. Rakibul Haque Rafid, M. Z. Hasan, and A. Karim, 'Brain Tumor Segmentation from 3D MRI Scans Using U-Net', *SN Comput. Sci.*, vol. 4, no. 4, p. 386, 2023, doi: 10.1007/s42979-023-01854-6.

[19] L. Zhang, A. Liu, J. Xiao, and P. Taylor, 'Dual Encoder Fusion U-Net (DEFU-Net) for Cross-manufacturer Chest X-ray Segmentation', in *2020 25th International Conference on Pattern Recognition (ICPR)*, 2021, pp. 9333–9339. doi: 10.1109/ICPR48806.2021.9412718.

[20] V. Basetti *et al.*, 'Economic Emission Load Dispatch Problem with Valve-Point Loading Using a Novel Quasi-Oppositional-Based Political Optimizer', *Electronics*, vol. 10, no. 21. 2021. doi: 10.3390/electronics10212596.

[21] A. Zhu, Z. Gu, C. Hu, J. Niu, C. Xu, and Z. Li, *Political optimizer with interpolation strategy for global optimization*, vol. 16, no. 5 May. 2021. doi: 10.1371/journal.pone.0251204.

[22] M. Zeybek, A. C. Universitesi, and L. Monitoring, 'Estimation of Powerline Route from Airborne', no. November, 2018.

[23] T. T. Nguyen *et al.*, 'Deep learning for deepfakes creation and detection: A survey', *Comput. Vis. Image Underst.*, vol. 223, p. 103525, 2022.

[24] H. Kibriya, M. Masood, M. Nawaz, R. Rafique, and S. Rehman, 'Multiclass brain tumor classification using convolutional neural network and support vector machine',

in *2021 Mohammad Ali Jinnah University international conference on computing (MAJICC)*, IEEE, 2021, pp. 1–4.
[25] M. Alnajjar, 'Image-based detection using deep learning and Google Colab', 2021.
[26] B. Koonce and B. E. Koonce, *Convolutional neural networks with swift for tensorflow: Image recognition and dataset categorization*. Springer, 2021.
[27] Q. Askari, I. Younas, and M. Saeed, 'Political Optimizer: A novel socio-inspired meta-heuristic for global optimization', *Knowledge-Based Syst.*, vol. 195, p. 105709, 2020, doi: https://doi.org/10.1016/j.knosys.2020.105709.